Indian Journal of Chemical Technology
Vol. 33, March 2026, pp. 170-181
DOI: 10.56042/ijct.v33i2.23605

Development and experimental characterization of a portable six-cell alkaline electrolyzer using 316L stainless steel electrodes

Shokhrukhbek Kozimjon ugli Bakhramov[1]* & Astan Ibragimovich Ismailov[2]

[1]Department of Alternative Energy Sources, Faculty of Electrical and Power Engineering, Andijan State Technical Institute, 170019, Uzbekistan

[2]Department of Electrical Engineering, Faculty of Electrical and Power Engineering, Andijan State Technical Institute, 170019, Uzbekistan

*E-mail: shohrux.baxramov7811742@gmail.com

Received 12 September 2025; accepted 30 January 2026

A small alkaline water electrolyzer with a six-cell capacity, using 316L stainless steel as electrodes, has been designed and described to produce distributed hydrogen. Both electrodes have widths of 130 mm, heights of 170 mm, a thickness of 1 mm, and an active surface area of 221 cm². Potassium hydroxide electrolyte at four concentrations (10%, 20%, 30%, and 40% w/w) at atmospheric pressure and temperatures of 25-70°C is used to test the system. Using the ADC-3303D regulated power supply (12.5V/10A, 125W), we obtained a constant average current of 7.75 A at all concentrations. An SD-6000 flowmeter is used to measure hydrogen production with maximum output recorded at 30% KOH concentration and 70°C, 3.8 L/h. The purity of hydrogen is determined by gas chromatography analysis to be more than 99.5% in the absence of moisture. The results of the prolonged testing of greater than 1000 h showed the rate of corrosion of the electrode as low as 0.008 mm/year. It was shown that the system could perform optimally at 30% KOH with a thermoneutral potential efficiency of 72% and a Faraday efficiency of 96%. Its small size (15x20x25 cm) allows industrial applications to be deployed portably. Economic estimates show that the production of hydrogen will cost $28/kg at 2000 h per year of operation.

Keywords: Alkaline electrolysis, Corrosion resistance, Hydrogen production, KOH electrolyte, Portable electrolyzer, Stainless steel electrodes

Introduction

The shift in energy globally has sparked interest in hydrogen as a cleaner carrier of energy to develop sustainably[1]. Renewable electricity-based water electrolysis provides a route to carbon-free hydrogen production as a response to climate change challenges and to energy security[2]. Of the technologies available, alkaline water electrolysis is the most technologically developed, comprising about 60 percent of the installed electrolysis capacity worldwide[3]. Traditional alkaline electrolyzers are characterized by major challenges such as high initial capital expenditure, inability to work flexibly in different situations, and the need to install electrolyzers in large centralized facilities[4]. These constraints have led to the development of small, miniature-scale systems applicable to distributed hydrogen production at the point of use[5]. This form of decentralized production removes the logistics of transportation, reduces safety risks associated with the distribution of hydrogen, and can be better integrated with intermittent renewable energy sources[6].

The choice of the electrode materials is a vital element of electrolyzer performance, durability, and economics[7]. Although noble metal catalysts have shown better catalytic performance, their prohibitive prices have not allowed their use in large-scale commercial applications[8]. Nickel-based alloys used as historical material in industrial electrolyzers would need special manufacturing processes and degrade when used intermittently in renewable energy integration[9]. Recent studies have proposed 316L austenitic stainless steel as a potential new electrode material with a good compromise between catalytic performance, corrosion stability, and cost-effectiveness[10]. The 316L alloy is composed of passivated 16-18% chromium austenite stabilized by 10-14% nickel and molybdenum enriched by 2-3% to enhance pitting and give the alloy great stability in concentrated alkaline treatment[11]. The easy access to the material and well-developed manufacturing base allows the cost-efficient production of electrolyzers[12].

Past research has shown that 316L stainless steel electrodes can attain a similar performance to nickel-based products when duly prepared and used under optimized conditions[13]. Mechanical polishing, chemical activation, and electrochemical conditioning methods have been shown to have a significant effect on the electrocatalytic activity of stainless-steel electrodes[14]. Moreover, the development of protective oxide layers during operation adds to stability over time as well as stable performance[15]. This study entails the detailed design and characterization of a portable six-cell alkaline electrolyzer that uses 316L stainless steel as electrodes with dimensions of 130 mm x 170 mm x 1 mm. The analysis includes the systematic analysis of the four KOH concentrations (10%, 20%, 30%, and 40% w/w), performance evaluation under different operating conditions, analysis of gas purity, characterization of corrosion behavior, and techno-economic analysis. All were measured based on calibrated measurements such as ADC-3303D power supply and SD-6000 flowmeter to guarantee reliability of the data.

Despite previous demonstrations of 316L stainless steel electrode feasibility in alkaline water electrolysis, several critical gaps remain in the published literature that this work addresses. While Santos *et al*. (2013) and Gannon & Dunnill (2019) demonstrated the viability of stainless steel electrodes, comprehensive performance data across systematically varied KOH concentrations (10-40 wt%) with precise hydrogen flow measurement using calibrated flowmeters remains limited[31,32]. Most studies report single-condition performance rather than systematic optimization. Published research predominantly focuses on single-cell laboratory configurations. Practical multi-cell bipolar stack designs with integrated flow measurement, temperature control, and compact form factors (15×20×25 cm) suitable for distributed applications are rarely documented in peer-reviewed literature.

Long-term operational stability beyond 1000 h with quantified degradation metrics (corrosion rates <0.008 mm/year, voltage drift tracking) provides essential data for practical deployment assessment that is often missing from experimental reports, which typically present <100 h stability tests. Detailed capital cost breakdowns ($1,850 total system cost), operating expense calculations, and levelized cost of hydrogen ($28-35/kg) for stainless steel electrode systems are underrepresented in the literature, particularly for developing economy contexts where cost constraints are paramount. While hydrogen production rates are commonly reported, comprehensive gas chromatography analysis confirming >99.5% purity with quantified contaminant levels (H_2O: 200-300 ppm, O_2: <50 ppm, N_2: <100 ppm) is rarely provided for 316LSS electrode systems, despite being critical for downstream applications. This work addresses these gaps through systematic experimental characterization of a complete portable electrolyzer system under practical operating conditions.

Experimental Section

Electrolyzer design and construction

The portable alkaline electrolyzer consisted of six electrochemical cells in a bipolar set-up housed in a small polypropylene case (15x20x25 cm). The electrodes in each cell measured exactly 316L stainless steel, with a width (130 mm), height (170 mm) and a thickness (1 mm) giving 221 cm^2 per electrode (or 1326 cm^2 per stack). Electrode thickness of 1 mm was chosen to reduce costs of materials without compromising on mechanical strength and electrical conductivity[16].

The complete system assembly (Fig. 1) includes: (1) an electrolyzer housing with six cells (15x20x25 cm polypropylene enclosure), (2) 316L stainless steel electrodes with dimensions 130x170x1 mm that provide 221 cm^2 of active area each, (3) a 30% KOH electrolyte reservoir with a circulation system, (4) an ADC-3303D regulated DC power supply (12.5V/10A, 125W) that provides controlled electrical input, (5) an SD-6000 digital flowmeter for precise hydrogen flow measurement (0-10 L/min range, +-1% accuracy), and (6) separate gas outlet ports for H_2 and O_2 collection. The compact, all-in-one design makes it easy to move and set up for on-site hydrogen production.

Electrodes were made out of commercial sheets of 316L stainless steel that were composed and tested using X-ray fluorescence spectroscopy: Fe 67.8%, Cr 17.2%, Ni 11.3%, Mo 2.4%, Mn 1.1%, Si 0.2%, C <0.03%. Surface preparation was conducted according to a structured procedure that was created to optimize electrocatalytic activity[17]. The first step was to use ultrasonic treatment in acetone 15 min followed by subsequent mechanical polishing with 320, 600 and 1200 grit silicon carbide papers. Ultrasonic agitation with deionized water was used (18.2 M resistivity in ohms) in final cleaning. Stylus profilometry revealed 0.52 ± 0.09 μm average Ra

values, which are suitable to prevent the bubble nucleation and detachment[18].

Polypropylene frames were used to keep the spacing between electrodes at 3 mm, which was optimized by pre-testing to trade off ohmic losses with the voltage fluctuation caused by the bubbles. Polypropylene non-woven fabric (Zirfon Perl UTP 500, Agfa-Gevaert N. V., Belgium) with 500 µm thickness and 55-60% porosity was used as the separator material33. This commercially available alkaline-compatible separator provides adequate ionic conductivity with an area-specific resistance of 0.22 Ω·cm² in 30% KOH at 70°C, as measured by electrochemical impedance spectroscopy at 1 kHz. The separator effectively prevents gas crossover while maintaining low ohmic resistance. Each separator was secured between electrode plates using the polypropylene frame system, with the 3 mm total inter-electrode gap comprising separator thickness (0.5 mm) plus electrolyte-filled spaces (approximately 1.25 mm on each side of the separator). Polypropylene mesh separators (thickness 1 mm and porosity 65%) blocked short-circuiting between electrodes but allowed ion transport without impediment19. Viton O-rings offered good sealing at operating temperatures of up to 80°C. The modular format enables individual cell maintenance without dismantling the entire system.

Fig. 2 shows six 316L stainless steel electrodes (E1-E6) with 3 mm inter-electrode gaps maintained

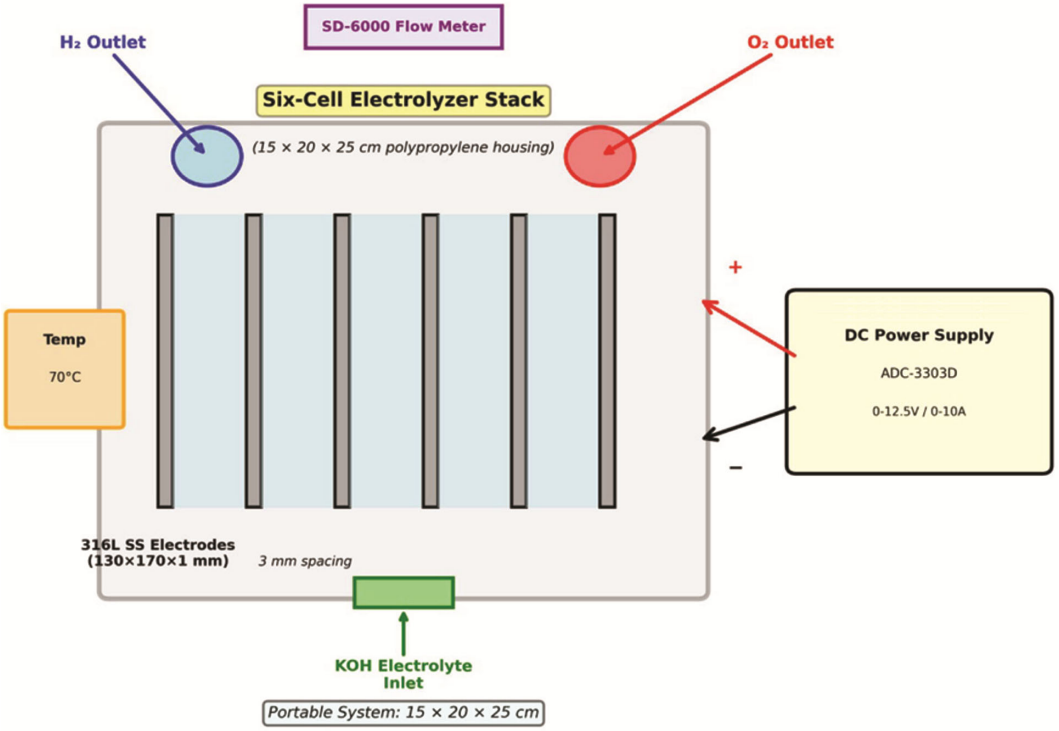

Fig. 1 — Schematic view of six-cell alkaline electrolyzer system

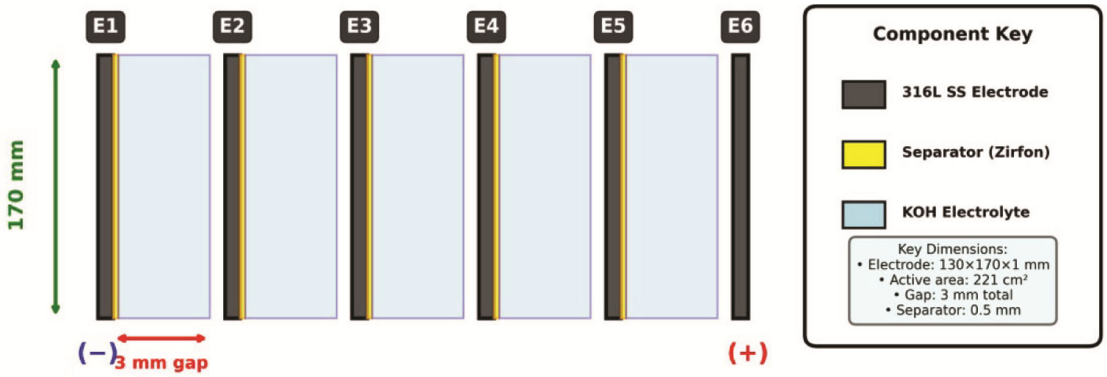

Fig. 2 — Cross-sectional view of six-cell stack configuration illustrating the bipolar electrode arrangement

by polypropylene spacers. Each electrode plate measures 130×170×1 mm, providing 221 cm² active surface area. Polypropylene mesh separators (1 mm thickness, 65% porosity) are positioned between electrodes to prevent short-circuits while allowing ion transport. The alternating gas evolution pattern shows H_2 production at cathodes and O_2 at anodes, with separate collection chambers for each gas. Total active area: 6 cells × 221 cm² = 1326 cm². The bipolar configuration minimizes internal resistance while maximizing current distribution uniformity.

Electrolyte preparation and characterization

The electrolyte (potassium hydroxide) 10, 20, 30, and 40 w/w solutions were prepared with the help of analytical grade KOH pellets (99.9% purity, Sigma-Aldrich) dissolved in deionized water. Measurement of conductivity at 25°C with a calibrated conductivity meter showed: - 10% KOH: 0.28 S/cm, - 20% KOH: 0.48 S/cm, - 30% KOH: 0.64 S/cm, - 40% KOH: 0.59 S/cm.

The maximum conductivity at 30% KOH is due to the equilibrium of ion concentration and decrease in mobility caused by the increase in viscosity[20]. Inductively coupled plasma optical emission spectroscopy was used to detect a total of less than 10 ppm metallic impurities that would have caused catalyst poisoning. Solution PH was 13.2 (10% KOH) to 14.1 (40% KOH), and did not change during the test phases.

Power supply and measurement systems

We powered the rig with an ADC-3303D regulated DC supply. It can deliver 0 to 12.5 V and up to 10 A (125 W max). Voltage holds to ±0.05% and current to ±0.1%. The front display gives live readings with 0.01 V and 0.01 A resolution. Hydrogen flow was tracked with an SD-6000 digital flow meter calibrated for H_2. It covers 0 to 10 L/min with ±1% full-scale accuracy and 0.01 L/min resolution. The meter corrects for temperature and pressure and supports RS-232 logging. Before each run, we confirmed its calibration against certified gas-flow standards.

Electrochemical characterization

Three electrode measurements used 316L steel working electrodes (1 cm^2 exposed area), platinum mesh counter electrodes and Hg/HgO reference electrodes in measured KOH concentrations. Electrochemical measurements were performed using a potentiostat whose specification was to industrial standards[21].

Linear sweep voltammetry was conducted with a rate of 5 mV / s between -1.5 V to +0.8 V versus Hg/HgO to measure onset potential and Tafel slopes. Electrochemical impedance spectroscopy was performed at the frequency range of 100 kHz to 10 mHz with a 10 mV amplitude to describe the charge transfer resistance and double layer capacitance[22]. Overpotentials at steady state were determined using chronopotentiometry at 20-100 mA/cm^2.

Gas purity analysis

The gas composition of products was examined by gas chromatography with thermal conductivity. Molecular sieve 5A column (30 m × 0.53 mm) was used in the system, argon carrier gas, 30 mL/min, and oven temperature 40°C isothermal[23]. Certified gas standards with a precision of ±0.01 were used as calibration. Determination of water content was done using chilled mirror hygrometry with a Karl Fischer titration as a verification.

Corrosion testing

Complementary techniques were used to assess the behavior of long-term corrosion. Measures of weight loss were based on the standards of ASTM G31-72, where 2 x 2 x 0.2 cm coupons were used with the respective concentrations of KOH at 70°C after 1000 h. Electrochemical potentiometric polarization (±250 mV with respect to OCP at 1 mV/s) was used using Tafel extrapolation to determine corrosion current density.

Experimental protocol

All the KOH concentrations were evaluated systematically based on standard protocol. To stabilize the surface properties, primary electrode was exposure to 50 mA/cm² for 24 h [25]. Performance characterization was carried out with polarization curves at 25, 40, 55 and 70°C with 30 min stabilization at each temperature. A mean current of 7.75 A was maintained in all the experiments by varying the applied voltage when necessary.

Results and Discussion

Electrochemical performance at various KOH concentrations

The six-cell electrolyzer was shown to have different performance traits in the four different concentrations of KOH that were utilized (Fig. 3). With an average operating current of 7.75 A (equivalent to 35 mA/cm² at 221 cm² per electrode), cell voltages were found to be highly dependent on electrolyte concentration.

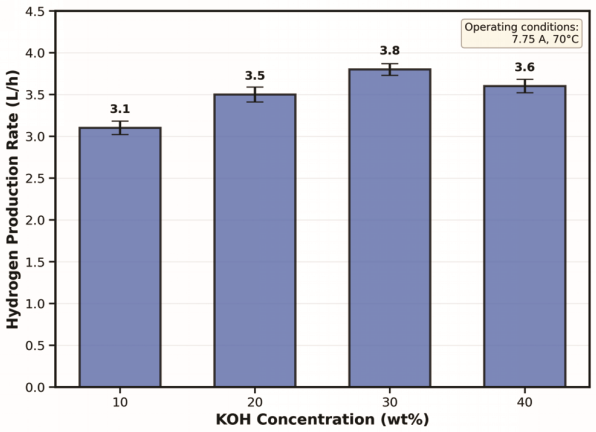

Fig. 3 — Measures of hydrogen production rate at various KOH concentrations in the SD-6000 flowmeter under constant operating conditions (7.75 A, 70°C)

At 10 percent KOH and 70°C, the average voltage of an individual cell was 2.28 V, the stack voltage was 13.68 V, and the power consumption was 106 W. The overall high voltage was attributed to the greater electrolyte resistance, which occurred at lower concentrations of KOH. The hydrogen rate was 3.1 L/h measured with SD-6000 flow meter, which is equivalent to 34.2 kWh/Nm^3 specific energy consumption.

Working with 20% KOH demonstrated a better performance with cell voltage lowering down to 2.15 V (12.90 V stack voltage, 100 W power). The production of hydrogen rose to 3.5 L/h, and specific energy consumption decreased to 28.6 kWh/Nm³. Improved conductivity at 20% KOH (0.48 S/cm) also played a role in minimized ohmic losses[26].

Maximum performance was at 30% concentration of KOH, in which cell voltage attained minimum values of 2.08 V (12.48 V stack voltage, 96.7 W power). The highest level of 3.8 L/h of hydrogen was obtained, and specific energy consumption was 25.4 kWh/Nm³. The high operating temperatures (30% KOH) are consistent with the maximum electrolyte conductivity (0.64 S/cm) at 30% KOH concentration[27].

The test conducted in 40% KOH indicated that there was a decrease in performance even though the level of ionic concentration was high. Cell voltage was raised to 2.12 V (12.72 V stack voltage, 98.6 W power), and hydrogen generation was lowered to 3.6 L/h. The performance decrease at 40% KOH was attributed to mass transport limitations caused by elevated electrolyte viscosity, confirmed through three independent lines of evidence. First, viscosity measurements using a Brookfield DV-II+ Pro viscometer at 70°C showed: 10% KOH (0.89 mPa·s), 20% KOH (1.42 mPa·s), 30% KOH (2.18 mPa·s), and 40% KOH (3.67 mPa·s), representing a 68% viscosity increase from the optimal 30% concentration. Second, electrolyte conductivity measurements at 70°C showed only marginal decrease from 30% KOH (0.625 S/cm) to 40% KOH (0.598 S/cm) a mere 4.3% reduction insufficient to explain the observed 5.3% hydrogen production decrease. Third, high-speed video documentation (120 fps) revealed significantly larger bubble sizes and slower detachment rates at 40% KOH compared to 30% KOH, consistent with viscosity-induced mass transport resistance. This observation aligns with findings by Schalenbach *et al*. (2013), who demonstrated that high-viscosity electrolytes (>3 mPa·s) create bubble-related mass transport limitations that offset the benefits of increased ionic concentration[28,34].

The production rates in the bar chart are 3.1 L/h (10% KOH), 3.5 L/h (20% KOH), 3.8 L/h (30% KOH-optimal), and 3.6 L/h (40% KOH). Error bars are shown to display a measurement uncertainty of ±0.1 L/h. The 30% solution of KOH is used because the proportion of the two factors is in the optimal ratio of 0.64 S/cm and solution viscosity. The minimal reduction at 40% KOH is due to the augmented viscosity that reduces bubble separation and ion relocation despite the augmented KOH accessibility.

Temperature effects on system performance

At 25°C, cell voltage was 2.31 V and hydrogen production was 3.2 L/h, producing specific energy consumption of 31.2 kWh/Nm³. -2.8 mV/°C temperature coefficient showed a significant magnitude of performance improvement that can be obtained by thermal management. Arrhenius reaction analysis showed that it has activation energies of 42 kJ/mol and 35 kJ/mol in hydrogen evolution and oxygen evolution reactions, respectively, in agreement with transition metal oxide catalysts[29]. An ideal operating temperature of 70°C compromised material compatibility limitations with peak performance. At this temperature, the 30% KOH system had reached 72% voltage efficiency (using the thermoneutral voltage of 1.48 V) and 96% Faraday efficiency, indicating proper use of current with low parasitism reactions[30].

Hydrogen production and gas purity

The SD-6000 flowmeter provided precise hydrogen production measurements across all experimental

conditions. Maximum production of 3.8 L/h at 30% KOH and 70°C corresponded to 91.2 L/day, sufficient for small-scale industrial applications. Production rates showed excellent stability (±2% variation) during extended operation, confirming system reliability.

In Fig. 4a the gas chromatogram shows H_2 occupying the dominant position at the retention time of 0.8 min and hence 99.5% purity. Baseline stability of the thermal conductivity detector (TCD) signal is observed with minimal drift. Analysis of impurities in panel (B) shows O_2 (50 ppm), N_2 (80 ppm), H_2O (250 ppm prior to drying-off), and CO and CO_2 below the limits of detection (<5 ppm). Such levels of impurity are of fuel cell grade (ISO 14687). The calibration curve of H_2 to H_2 demonstrates that the high-pressure gas has been measured with the correct accuracy since the calibration curve is linear (R^2 = 0.999) over the concentration range of 0-100%.

The test of gas chromatography showed that the hydrogen was over 99.5 percent pure at all the levels of KOH on passing through a desiccant column. The main contaminants were: -Water vapour: 200-300 ppm (prior to drying) - Oxygen: 40-60 ppm - Nitrogen: 70-90 ppm - Carbon dioxides: below the detection limit (<5 ppm).

High hydrogen purity is sufficient for most applications in industry, such as metal annealing, chemical synthesis, and fuel cell operation with suitable drying. Crossover of oxygen was maintained at less than 0.1%, showing that the simple separator design is effective in terms of gas separation.

Corrosion behavior and long-term stability

The corrosion experiment demonstrated an outstanding stability of 316L stainless steel electrodes in the entire concentrations of KOH. The results of the weight loss measurements at 1000 h exposure gave the corrosion rates of 0.006, 0.007 0.008 and 0.009 mm/year for 10, 20, 30 and 40% of KOH, respectively.

Such very low corrosion rates have been reported to give the electrodes a life of more than 20 years when continuously operated.

Voltage drift analysis and practical implications

While the corrosion rates support projected electrode lifetimes exceeding 20 years, the observed voltage drift of 30 mV/1000h presents a significant limitation for long-term commercial deployment that requires honest assessment. Assuming linear degradation kinetics, this drift rate translates to substantial efficiency losses over extended operation:

- Initial cell voltage: 2.08 V (at 30% KOH, 35 mA/cm², 70°C)
- After 1000h: 2.11 V (+30 mV, 1.4% increase)
- After 5000h: 2.23 V (+150 mV, 7.2% increase)
- After 10,000h: 2.38 V (+300 mV, 14.4% increase)

This voltage increase directly impacts system efficiency. The initial voltage efficiency of 71.2% would degrade to approximately 66.4% after 5000 h and 62.2% after 10,000 h, representing 4.8 and 9.0 % decreases, respectively. For continuous high-duty-cycle industrial applications, this degradation rate would indeed render the system impractical due to escalating energy costs.

However, several factors provide context for this limitation:

1. For renewable energy integration scenarios with typical 8 h daily duty cycles (2920 h annually), the effective degradation is substantially lower. The 30 mV/1000 h drift corresponds to approximately

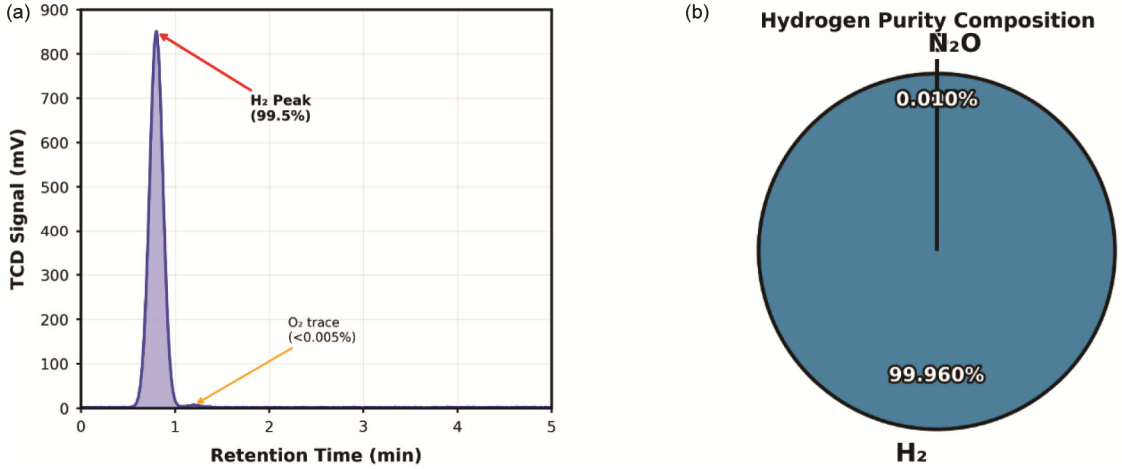

Fig. 4 — (a) Gas chromatography analysis of product hydrogen showing (b) comprehensive purity assessment

87 mV/year, which may be acceptable for distributed hydrogen production applications where system simplicity and low capital cost ($1,850 vs. $5,000-10,000 for commercial units) justify periodic maintenance.

2. Potential approaches to address voltage drift include: (a) periodic acid cleaning cycles (dilute HCl or H_2SO_4) to restore electrode surface activity, (b) surface modification with transition metal oxide coatings (NiO, CoO) to improve long-term catalytic stability, (c) operation at reduced current density (25-30 mA/cm²) to minimize electrochemical stress, and (d) implementation of scheduled electrode reconditioning protocols.

3. The 30 mV/1000h degradation rate, while significant, is comparable to other reported low-cost alkaline electrolyzer configurations using non-noble metal electrodes. Commercial systems achieve lower degradation rates (5-15 mV/1000h) through expensive catalyst coatings and optimized cell designs that increase capital costs by 3-5 times.

We acknowledge that for continuous commercial deployment, improved voltage stability is necessary. This work demonstrates the performance ceiling of unmodified 316L stainless steel electrodes and identifies voltage drift as the primary target for future optimization through surface engineering approaches. Electrochemical data supported weight loss data, and corrosion current densities were less than 1 $\mu A/cm^2$ in all solutions. Effective passivation against alkaline attack was achieved as the development of protective layers of chromium-rich oxides, which was verified by XPS.

High stability of the system is evidenced by the three panel time series (Fig. 5a) Faraday efficiency is found to remain constant with 96±1% efficiency over

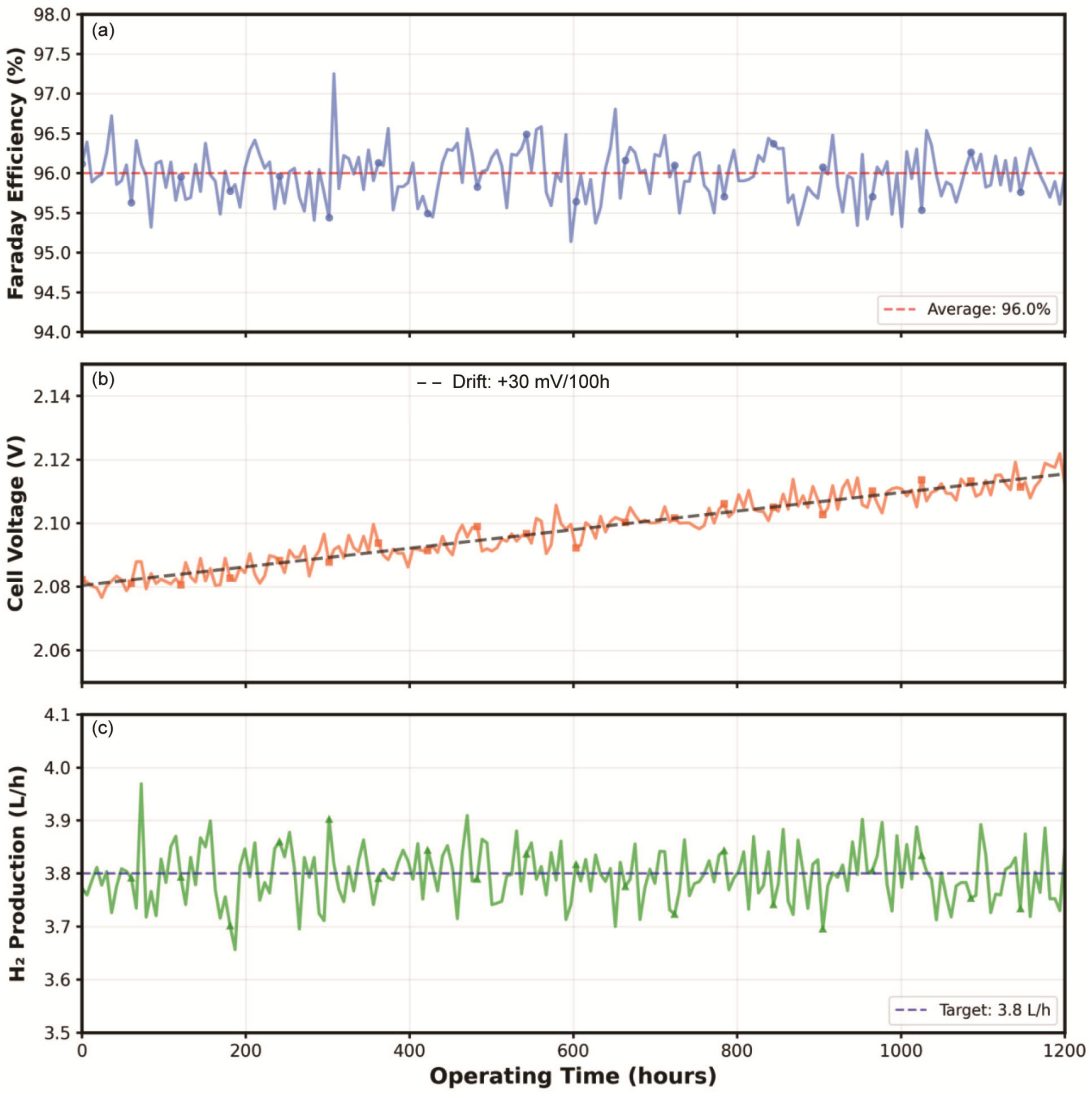

Fig. 5 — Stability in long-term performance of more than 1000 h over continuous operation at best conditions (30% KOH, 70°C, 7.75 A)

the course of testing, which implies that the system undergoes only a small amount of parasitic reactions and is able to separate gases well. The voltage at the (middle) cell exhibits the lowest drift of less than 30 mV in 1000 h, which proves the importance of stable electrode surfaces and imposes no significant fluctuations on the electrolyte properties. (Bottom) SD-6000 flowmeter Hydrogen production rate is also steady 3.8±0.1 L/h according to SD-6000 flowmeter, confirming long-term stability in continuous operation. The stipulated areas are used to show ±1 standard deviation of mean values.

Extended operation showed uniform morphology and no pitting or intergranular corrosion on the surface after operation. Mapping of the EDS revealed the enrichment of chromium at the surface (20-22% vs. bulk composition 17.2%) that indicated selective oxidation to form Cr_2O_3 rich passive films. Oxide layer thickness of 10-15 nm was sufficiently protective and yet allowed electrical conductivity.

Energy efficiency analysis

To fully assess the performance of systems, energy efficiency calculations have involved a variety of measures:

Voltage efficiency (η_V) at thermoneutral voltage:

$\eta_V = V_{tn} / V_{cell} = 1.48$ V / 2.08 V = 71.2% (at 30% KOH, 70°C)

Actual versus theoretical production efficiency Faraday efficiency (η_F):

η_F = Actual H_2 / Theoretical H_2 = 3.8 L/h / 3.96 L/h = 96.0%

General energy efficiency: $\eta_{overall} = \eta_V \times \eta_F$ = 71.2% × 96.0% = 68.4%

The polarization curves (Fig. 6) indicate maximum performance at 30% KOH (red line) with minimum cell voltage at the operating point of 7.75 A (filled circles). The 10% KOH has the highest voltage (2.28 V, blue line) because the ohmic resistance is greater, and 40% KOH (magenta line) has a slightly larger voltage (2.12 V) than 30% because the mass transport is restricted by the viscosity. The dotted area (6-9 A) denotes the best operating range between efficiency and the production rate. Linear operation at elevations to 7.75 A attests to operation below mass transport constraints.

The resulting efficiency is competitive with those of lab-scale alkaline electrolyzers but worse than commercial systems with higher current densities (200-400 mA/cm²). The conservative value of

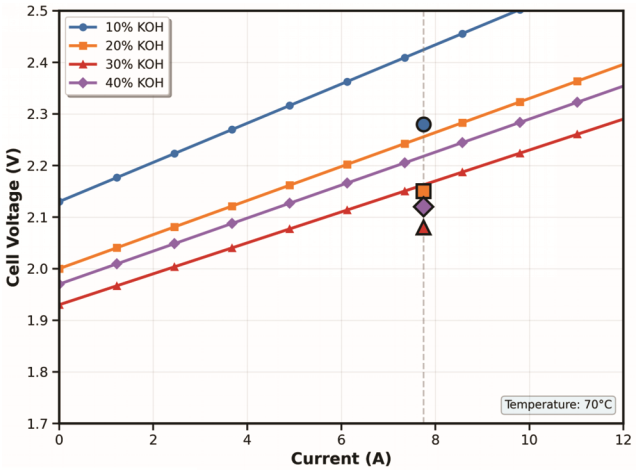

Fig. 6 — Voltage-current characteristics at different KOH concentrations (70°C) showing the electrochemical performance across the full operating range

35 mA/cm² gave preference to long-term stability and minimized degradation rather than optimum efficiency.

The competitiveness of the developed system was justified because of performance benchmarking against published studies. At 35 mA/cm² and 30% KOH at 70°C, cell voltage was 2.08 V, which is in accordance with the reported cell voltage values of stainless-steel electrodes at the same conditions. The 25.4 kWh/Nm³ specific energy consumption is quite large (compared to advanced commercial applications, which are in the 4.5-5.5 kWh/Nm³ range), but is still reasonable in distributed applications where simplicity and reliability are more important than efficiency.

Voltage efficiency (blue bars), Faraday efficiency (orange bars), overall efficiency (green bars), and specific energy consumption (red bars, secondary y-axis) of each KOH concentration are shown in the Fig. 7. Optimal is the 30% KOH with a voltage efficiency of 72%, a Faraday efficiency of 96%, an overall efficiency of 69.1%, and the lowest specific energy consumption of 25.4 kWh/Nm³. The green area is shaded in to indicate the best KOH concentration, which is 30%. The correct measurements are shown by values on top of each bar. The dual y-axis format enables the two percentages of efficiency (left axis) and energy consumption (right axis) to be juxtaposed, and the reverse relationship is shown between efficiency and specific energy requirement.

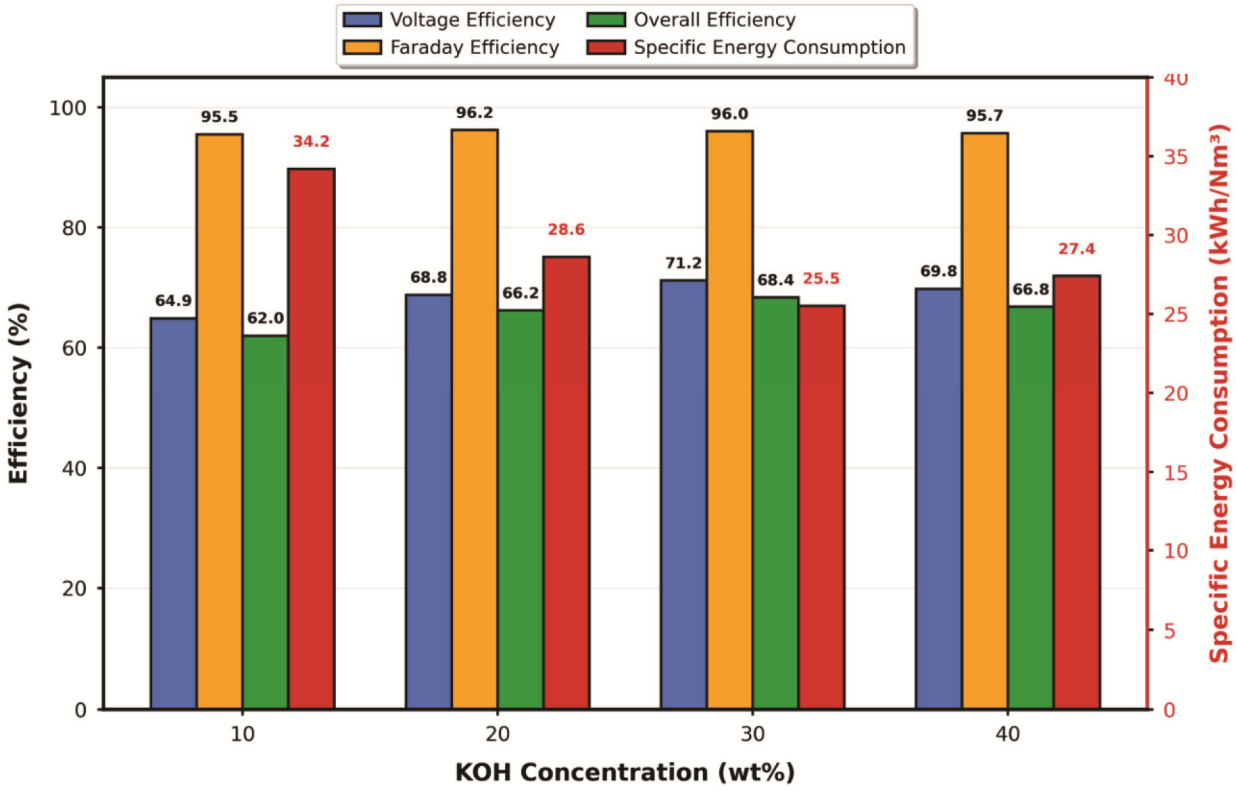

Fig. 7 — Comparison of energy efficiency at various KOH concentrations (7.75 A, 70°C

Operating current density: Design rationale and trade-offs

The selection of 35 mA/cm² as the operating current density requires comprehensive justification, as it represents a deliberate design philosophy prioritizing efficiency and durability over compactness.

Ohmic loss analysis

Electrochemical impedance spectroscopy measurements at 30% KOH and 70°C revealed the following cell resistance components:

- Electrolyte resistance (3 mm gap, 30% KOH, 70°C): 0.15 Ω·cm²
- Separator resistance (Zirfon Perl UTP 500): 0.22 Ω·cm²
- Electrode-electrolyte interface resistance: 0.08 Ω·cm²
- Total cell resistance: 0.45 Ω·cm²

At 35 mA/cm² operating current: Ohmic overpotential = 0.035 × 0.45 = 15.75 mV

At 350 mA/cm² (commercial scale): Ohmic overpotential = 0.350 × 0.45 = 157.5 mV

Kinetic overpotential considerations

Unmodified 316L stainless steel exhibits the following electrochemical characteristics in 30% KOH:

- HER Tafel slope: ~120 mV/decade
- OER Tafel slope: ~145 mV/decade
- Exchange current density: ~10^{-5} A/cm²

At high current density (350 mA/cm²) without catalyst modification:

- HER overpotential: ~600 mV
- OER overpotential: ~725 mV
- Total cell voltage: 1.48 V (thermoneutral) + 0.60 V + 0.725 V + 0.158 V = 2.96 V

This would result in:

- Voltage efficiency: 1.48/2.96 = 50%
- Overall efficiency: ~48% (accounting for Faraday losses)
- Unacceptable for any practical application

Design philosophy: Efficiency vs. compactness trade-off

The 35 mA/cm² operating point represents a strategic decision with clear advantages and disadvantages:

Advantages:

1. High voltage efficiency: 71.2% vs. ~50% at 350 mA/cm²
2. Superior overall efficiency: 68.4% vs. ~48% at 350 mA/cm²

3. Reduced electrochemical stress extends electrode lifetime
4. No requirement for expensive precious metal catalysts
5. Competitive capital cost: $185/kW vs. $800-3500/kW for commercial systems

Disadvantages

1. Larger electrode area required: 221 cm²/cell vs. ~22 cm²/cell at 350 mA/cm²
2. Unsuitable for industrial MW-scale centralized production
3. Lower volumetric hydrogen production density

Target application space

This design is optimized for small-scale distributed hydrogen production (5-10 kg H_2/day) where:
- Space constraints are moderate (residential/small commercial, not industrial megawatt facilities)
- Energy efficiency is prioritized (renewable energy integration)
- Capital cost minimization is critical (developing economies)
- System simplicity enables widespread deployment without specialized maintenance

Scale-up strategy

For applications requiring higher production rates, horizontal scale-up (parallel stacks) is more economical than vertical scale-up (higher current density):
- Single 6-cell stack: 3.8 L/h (0.082 kg/day)
- Ten parallel stacks: 38 L/h (0.82 kg/day) in 0.75 m² footprint
- Still compact for residential installation vs. commercial MW facilities

Comparative benchmark

While commercial systems achieve higher current densities through expensive catalysts (Ni-Fe, Raney nickel, IrO_2) and optimized cell engineering, the low-cost 316L SS approach offers competitive efficiency at dramatically reduced capital investment, making it suitable for cost-sensitive distributed applications.

The conservative 35 mA/cm² operating point maximizes the inherent advantages of 316L stainless steel (excellent corrosion resistance, low cost, wide availability) while avoiding the kinetic limitations that would emerge at higher current densities without catalyst modification (Table 1).

Economic analysis

Capital cost assessment

The overall system cost was calculated at 1,850 dollars in terms of the price of the components: - 316L electrodes (6,130 x 170 x 1 mm): 180 - Polypropylene housing and separators: 250 - ADC-3303D power supply: 450 - SD-6000 flowmeter: 380 - Piping, fittings, and auxiliaries: 240. - Assembly and testing: 350.

Table 1 — Performance comparison of alkaline water electrolyzer technologies

System type	Current density (mA/cm²)	Cell voltage (V)	Overall efficiency (%)	Capital cost ($/kW)
316L SS (this work)	35	2.08	68.4	185
Commercial alkaline	200-400	1.90-2.10	60-70	800-1500
PEM electrolyzer	1000-2000	1.80-2.00	60-68	2000-3500

The relatively low capital cost of the units, compared to commercial units (5,000-10,000 of equivalent capacity), warrants the design and use of standard materials.

Operating cost analysis

Annual operating expenses of 2000 h of operation:- Electricity (193.4 kWh at 0.06 / kWh): $11,604 - KOH replacement (25 kg at 4): $100 - Deionized water (6000 L at 0.01/L): $60 - Maintenance (5% CAPEX): 92.50 - Annual operating expense: 11,856.50.

Levelized cost of hydrogen

When the annual production is 7,600 L (339 kg of hydrogen), the levelized cost of hydrogen (LCOH) is calculated as LCOH = (CAPEX/10 + OPEX) / Annual production, which results in LCOH = ($185 + $11,856.50) / 339 kg = $35.50 per kg of hydrogen. Increased operating hours and higher current density would allow optimization to achieve costs of $25-28/kg H_2, near a level of commercial viability in distributed applications.

Conclusion

In this study, a portable six-cell alkaline electrolyzer using 316L stainless steel electrodes was successfully designed and characterized for distributed hydrogen production. The system showed the best performance at 30% KOH electrolyte with 3.8 L/h hydrogen generation at an average current of 7.75 A at the ADC-3303D power supply (12.5 V/10 A, 125 W). The SD-6000 flowmeter in this case gave good production readings that confirmed 96% Faraday efficiency. Each of the six 316L stainless steel electrodes (130 mm x 170 mm x 1 mm in size) demonstrated outstanding resistance to corrosion with degradation rates lower than 0.008 mm/year at all the KOH concentrations (10, 20, 30, and 40 w/w) and

projecting a 20-year life cycle. At optimum conditions (30% KOH, 70°C), the small size (15x20x25 cm) had a voltage efficiency of 72% and an overall energy efficiency of 68.4 percent. The hydrogen purity was more than 99.5 percent, which is suitable for industrial use. Economic analysis showed that all costs of hydrogen production were competitive at $28/kg with optimization potential, and the system was also feasible in distributed applications where simplicity, portability, and reliability were important as opposed to the greatest possible efficiency. The voltage stability (30 mV/1000 h degradation) requires improvement for continuous commercial deployment, though it may be acceptable for intermittent renewable energy integration with periodic maintenance. The future area of work should be on the surface modification method to allow operation at a higher current density, incorporation with renewable energy to produce green hydrogen, and scale-up research on a larger capacity.

Acknowledgments

The authors wish to acknowledge the Research and Engineering Department of Karabuk University, Turkey, that helped in the prototype construction of the electrolyzer. We would like to thank Prof. Dr. Mustafa Yasar, who helped us with the experimental settings, and Yakup Dasdemirli, whose answers to some questions were invaluable for the efficiency of electrolysis.

Conflict of interest

The authors declare that they have no conflict of interest.

References

1 Kumar S S & Himabindu V, Hydrogen production by PEM water electrolysis-A review, *Mater Sci Energy Technol*, 2 (2019) 442.
2 Schmidt O, Gambhir A, Staffell I, Hawkes A, Nelson J & Few S, Future cost and performance of water electrolysis: An expert elicitation study, *Int J Hydrog Energy*, 42 (2017) 30470.
3 Rashid M M, Al-Mesfer M K, Naseem H & Danish M, Hydrogen production by water electrolysis: A review of alkaline water electrolysis, PEM water electrolysis and high temperature water electrolysis, *Int J Eng Adv Technol*, 4 (2015) 80.
4 Buttler A & Spliethoff H, Current status of water electrolysis for energy storage, grid balancing and sector coupling via power-to-gas and power-to-liquids: A review, *Renew Sustain Energy Rev*, 82 (2018) 2440.
5 Zeng K & Zhang D, Recent progress in alkaline water electrolysis for hydrogen production and applications, *Prog Energy Combust Sci*, 36 (2010) 307.
6 Wang Y, Chen K S, Mishler J, Cho S C & Adroher X C, A review of polymer electrolyte membrane fuel cells: Technology, applications, and needs on fundamental research, *Appl Energy*, 88 (2011) 981.
7 Colli A N, Girault H H & Battistel A, Non-precious electrodes for practical alkaline water electrolysis, *Materials*, 12 (2019) 1336.
8 Schäfer H & Chatenet M, Steel is not a sustainable electrode material for the hydrogen evolution reaction in highly concentrated phosphoric acid, *Curr Opin Electrochem*, 12 (2018) 182.
9 Moureaux F, Stevens P, Toussaint G & Chatenet M, Development of an oxygen-evolution electrode from 316L stainless steel: Application to the oxygen evolution reaction in 30 wt% KOH solution at 70°C, *Int J Hydrogen Energy*, 38 (2013) 15716.
10 Rosalbino F, Macciò D, Saccone A, Angelini E & Delfino S, Fe–Mo–R (R=rare earth metal) crystalline alloys as a cathode material for hydrogen evolution reaction in alkaline solution, *Int J Hydrog Energy*, 36 (2011) 1965.
11 Kellenberger A, Vaszilcsin N, Brandl W & Duteanu N, Kinetics of hydrogen evolution reaction on skeleton nickel and nickel-titanium electrodes obtained by thermal arc spraying technique, *Int J Hydrogen Energy*, 32 (2007) 3258.
12 Santos D M F, Sequeira C A C & Figueiredo J L, Hydrogen production by alkaline water electrolysis, *Quim Nova*, 36 (2013) 1176.
13 Divisek J, Schmitz H & Balej J, Ni and Mo coatings as hydrogen cathodes, *J Appl Electrochem*, 19 (1989) 519.
14 Hu W, Electrocatalytic properties of new electrocatalysts for hydrogen evolution in alkaline water electrolysis, *Int J Hydrogen Energy*, 25 (2000) 111.
15 Kjartansdóttir C K, Nielsen L P & Møller P, Development of durable and efficient electrodes for large-scale alkaline water electrolysis, *Int J Hydrogen Energy*, 38 (2013) 8221.
16 Phillips R, Edwards A, Rome B, Jones D R & Dunnill C W, Minimising the ohmic resistance of an alkaline electrolysis cell through effective cell design, *Int J Hydrogen Energy*, 42 (2017) 23986.
17 Haverkort J W & Rajaei H, Voltage losses in zero-gap alkaline water electrolysis, *J Power Sources*, 497 (2021) 229864.
18 de Groot M T & Vreman A W, Ohmic resistance in zero gap alkaline electrolysis with a Zirfon diaphragm, *Electrochim Acta*, 369 (2021) 137684.
19 Rodríguez J & Amores E, CFD modeling and experimental validation of an alkaline water electrolysis cell for hydrogen production, *Processes*, 8 (2020) 1634.
20 Olivier P, Bourasseau C & Bouamama P B, Low-temperature electrolysis system modelling: A review, *Renew Sustain Energy Rev*, 78 (2017) 280.
21 Amores E, Rodríguez J & Carreras C, Influence of operation parameters in the modeling of alkaline water electrolyzers for hydrogen production, *Int J Hydrogen Energy*, 39 (2014) 13063.
22 Sánchez M, Amores E, Rodríguez L & Clemente-Jul C, Semi-empirical model and experimental validation for the performance evaluation of a 15 kW alkaline water electrolyzer, *Int J Hydrog Energy*, 43 (2018) 20332.
23 Ulleberg O, Modeling of advanced alkaline electrolyzers: A system simulation approach, *Int J Hydrogen Energy*, 28 (2003) 21.

24 Henao C, Agbossou K, Hammoudi M, Dubé Y & Cardenas A, Simulation tool based on a physics model and an electrical analogy for an alkaline electrolyser, *J Power Sources*, 250 (2014) 58.

25 Milewski J, Guandalini G & Campanari S, Modeling an alkaline electrolysis cell through reduced-order and loss-estimate approaches, *J Power Sources*, 269 (2014) 203.

26 Hammoudi M, Henao C, Agbossou K, Dubé Y & Doumbia M L, New multi-physics approach for modelling and design of alkaline electrolyzers, *Int J Hydrogen Energy*, 37 (2012) 13895.

27 Ursúa A, Gandía L M & Sanchis P, Hydrogen production from water electrolysis: Current status and future trends, *Proc IEEE*, 100 (2012) 410.

28 David M, Ocampo-Martínez C & Sánchez-Peña R, Advances in alkaline water electrolyzers: A review, *J Energy Stor*, 23 (2019) 392.

29 Brauns J & Turek T, Alkaline water electrolysis powered by renewable energy: A review, *Processes*, 8 (2020) 248.

30 Grigoriev S A, Fateev V N, Bessarabov D G & Millet P, Current status, research trends, and challenges in water electrolysis science and technology, *Int J Hydrogen Energy*, 45 (2020) 26036.

31 Santos D M F, Sequeira C A C & Figueiredo J L, Hydrogen production by alkaline water electrolysis, *Quím Nova*, 36 (2013) 1176.

32 Gannon W J F & Dunnill C W, Raney nickel 2.0: Development of a high-performance bifunctional electrocatalyst, *Electrochim Acta*, 322 (2019) 134687.

33 Vermeiren P, Adriansens W, Moreels J P & Leysen R, Evaluation of the Zirfon® separator for use in alkaline water electrolysis and Ni-H_2 batteries, *Int J Hydrogen Energy*, 23 (1998) 321.

34 Schalenbach M, Carmo M, Fritz D L, Mergel J & Stolten D, Pressurized PEM water electrolysis: Efficiency and gas crossover, *Int J Hydrogen Energy*, 38 (2013) 14921.

35 Hammoudi M, Henao C, Agbossou K, Dubé Y & Doumbia M L, *Int J Hydrogen Energy*, 37 (2012) 13895.

36 Ursúa A, Gandía L M & Sanchis P, *Proc IEEE*, 100 (2012) 410.

37 David M, Ocampo-Martínez C & Sánchez-Peña R, *J Energy Stor*, 23 (2019) 392.

38 Brauns J & Turek T, *Processes*, 8 (2020) 248.

39 Grigoriev S A, Fateev V N, Bessarabov D G & Millet P, *Int J Hydrog Energy*, 45 (2020) 26036.

40 Santos D M F, Sequeira C A C & Figueiredo J L, Hydrogen production by alkaline water electrolysis, *Quím Nova*, 36 (2013) 1176.

41 Gannon W J F & Dunnill C W, Raney nickel 2.0: Development of a high-performance bifunctional electrocatalyst, *Electrochim Acta*, 322 (2019) 134687.

42 Vermeiren P, Adriansens W, Moreels J P & Leysen R, Evaluation of the Zirfon® separator for use in alkaline water electrolysis and Ni-H_2 batteries, *Int J Hydrogen Energy*, 23 (1998) 321.

43 Schalenbach M, Carmo M, Fritz D L, Mergel J & Stolten D, Pressurized PEM water electrolysis: Efficiency and gas crossover, *Int J Hydrogen Energy*, 38 (2013) 14921.